A flow network formulation for compressible and incompressible flow

J.J. Pretorius, A.G. Malan and J.A. Visser
Department of Mechanical & Aeronautical Engineering, University of Pretoria, Pretoria, South Africa

Received 5 December 2005
Revised 2 January 2007
Accepted 2 February 2007

Abstract

Purpose – One-dimensional pipe network flow analysis can be used in many applications to satisfactorily solve various engineering problems. The paper aims to focus on this.

Design/methodology/approach – A hybrid nodal method is detailed, which solves the pressure field prior to the elemental flows, and models both compressible gas and incompressible liquid and gas flows.

Findings – The results obtained by the algorithm were verified against a number of published benchmark flow problems. The methodology was found to yield accuracy similar or improved, compared with that of others, while being applicable to both incompressible liquid and compressible gas flows. Convergence performance was found to be similar to other hybrid techniques.

Originality/value – All flows are modelled via a single governing equation set. In the case of incompressible flow, the method is capable of dealing with both constant and variable cross-sectional area ducts. The latter includes geometrically complex pipes such as sudden expansions.

Keywords Pipes, Gas flow, Liquid flow, Simulation

Paper type Research paper

Nomenclature

A = cross sectional area (m^2)
c = flow loss coefficient, $c = c(K)$
d = external mass flow (kg/s)
D = diameter (m)
E = total number of pipe elements
F = friction factor
H = flow directional change denominator
I = total number of nodes in a pipe network mesh
J = number of pipe elements surrounding a specific node
K = flow loss correlation
L = pipe/elemental length (m)
M = Mach number
$\dot{m}$ = mass flow (kg/s)
$\mathbf{n}$ = normal vector
p = average static pressure (Pa)
Q = elemental volume flow (m^3/s)
R = ideal gas constant ($m^2/(s^2 K)$)
s = initial flow direction indicator
T = temperature (K)
u = pipe/element cross-sectional average velocity (m/s)
V = total elemental volume (m^3)

Greek
α = relaxation parameter
β = group of terms
γ = specific heat ratio
δ = gas/fluid type selector
ε = convergence parameter
ρ = pipe/element cross-sectional average density
φ = denominator: group of terms

Supercript
$*$ = last/guessed numerical value
$'$ = corrected numerical value

Subscript
ag = gas term indictor for equation of state
i = node/vertex point

International Journal of Numerical Methods for Heat & Fluid Flow
Vol. 18 No. 2, 2008
pp. 185-201

0961-5539
DOI 10.1108/09615530810846338

j	= adjacent node/vertex point to i	dyn	= dynamic component
f	= flow losses	s	= static component
x	= Cartesian coordinate aligned with axis of pipe element	a	= denominator
0	= total pressure	PFE	= pressure drop-flow equation

1. Introduction

The simulation of flow in pipe networks has found applicability in the design of natural gas and water distribution or the pipeline transport industry (Osiadacz, 1988; Potter and Wiggert, 1991). In addition, various other engineering flow problems may be solved using this 1D approach. For example, the flow of air through complex geometries may be analysed to first-order accuracy with little effort by using a 1D simulation to connect different flow paths together. A novel example of such an application, is the preliminary design of airflow through a gas turbine combustor chamber (Stuttaford and Rubini, 1996; Pretorius, 2004). In thus, pipe network simulation holds true potential as an engineering design tool. Ideally such a tool should be able to deal with both compressible gas and incompressible gas and liquid flows in variable cross-sectional area ducts. A number of pipe network numerical methods at present exist viz. nodal, loop and hybrid methods.

The nodal method utilizes the continuity equation to establish a mass balance at each node of the network, which is solved simultaneously to yield element flows. The pressure change over elements is provided via a pressure drop-flow relationship, which follows from the flow momentum equations. The advantage of nodal methods lies in the fact that the formulation is relatively straightforward to implement into numerical code, while requiring less storage space than element-based methods. There is also no need to specify loops or carefully selected initial flows as with the loop-based method. The nodal approach can further deal with mixed boundary conditions consisting of either pressure or flow. The main disadvantage of this method is however the poor convergence characteristic that it poses, as well as its extreme sensitivity to initial guessed pressure values (Osiadacz, 1988; Potter and Wiggert, 1991).

The loop method uses the same basic set of equations as the nodal method but with different boundary conditions (Osiadacz, 1988, 1987). A number of loops, representing the flow through a network, are however constructed. Kirchoff's second law, which is that the sum of the pressure-drops around any loop equals zero, is then applied. The advantage of this method is that the storage requirement is lower as compared to the other methods and it further also poses very good convergence characteristics. The main disadvantage is the necessity to define loops, of which the appropriate choice (from a numerical point of view) is not necessarily trivial (Osiadacz, 1987).

The hybrid pipe network method (Osiadacz, 1987; Greyvenstein and Laurie, 1994; Greyvenstein, 2002) combines aspects of the nodal and loop-based techniques, and such that the advantages of these approaches are inherited. The nodal aspect of the formulation makes the network definition much easier and yields a sparser matrix, while the good convergence characteristics of the loop formulation are preserved (Osiadacz, 1988, 1987). Amongst the hybrid methods, is a technique pioneered by Greyvenstein and Laurie (1994), which makes use of the SIMPLE pressure correction technique developed by Patankar (1980). Their formulation is shown to effectively simulate incompressible flow (Greyvenstein and Laurie, 1994) as well as compressible flows at Mach numbers of up to 0.7 (Greyvenstein, 2002). In the aforementioned work, separate governing equations are however solved for compressible gas and incompressible liquid flows.

In the interest of the generic applicability of a pipe network modelling tool, it would however be more advantageous to employ a single continuity and momentum equation set which describes flows ranging from incompressible to highly compressible. Networks or even single elements containing both flow types may thereby be solved effectively. Further, the method employed in existing work to construct the pressure correction equation (Greyvenstein and Laurie, 1994; Greyvenstein, 2002) requires the analytical and/or numerical differentiation of a number of terms, making the method potentially cumbersome to implement into computer code. Finally, nowhere in the literature are current hybrid approaches applied to model axisymmetric ducts with discontinuous changes in cross-sectional flow area (sudden expansion or contraction) via a single pipe element without employing a specialised formulation.

In this paper, a hybrid pipe network method based on the work of Greyvenstein and Lauries (1994) is proposed. It however employs a single equation set to describe both steady incompressible as well as highly compressible flows. In addition, the model has the capability to compute flows through variable area ducts with discontinuous changes in cross-sectional area in the case of incompressible flow. The differentiation of flow-related nonlinearities such as flow friction are further dealt with in a straightforward manner when constructing the pressure correction equation. It will be shown via the simulation of a number of benchmark problems, that the resulting methodology yields accurate results in all cases. It will further be shown to offer improved accuracy as compared to that of others for certain flows, and at no additional computational cost.

2. Governing equations

The governing equations to be satisfied in a steady isothermal fluid network are the continuity, pressure drop-flow rate and density equations. The latter is the equation of state in the case of gasses. The strong form for the continuity equation for 1D flow, as may be applied to a pipe network, is as follows:

$$\frac{\partial}{\partial x}(\rho u) = 0 \tag{1}$$

where ρ and u, respectively, denote the cross-sectional average density and velocity at a point along a 1D pipe element. The momentum equation, in the absence of gravitational effects, reduces to the following:

$$\frac{\partial p}{\partial x} + \frac{\partial}{\partial x}(\rho u^2) = \xi \tag{2}$$

where p is the element cross-sectional average static pressure, $\xi = u^2 c_f$ denotes a product between the average cross-sectional area velocity u and the drag coefficient c_f. The latter accounts for the effect of flow frictional losses where $c_f(K)$ is typically a function of flow loss correlation ($K(u)$) which is obtained analytically or from experimental data.

Densities for both compressible gasses (ideal) and liquids are in this work computed by utilizing the following single relation:

$$\rho_a = \delta_{ag}\frac{p_a}{RT_a} + (1-\delta_{ag})\rho_{al}(T_a) \tag{3}$$

where:

$$\delta_{ag} = \begin{cases} 0 & \text{for liquids} \\ 1 & \text{for ideal gasses} \end{cases}$$

Here, δ is the Kronecker delta, $a = \text{g}$ denotes gas and in the case of a liquid $a = \text{l}$. Further, R is the ideal gas constant and T is the temperature. The temperatures are provided as a boundary condition in this work as thermal energy conservation is not explicitly solved for.

3. Discretization procedure

In the paragraphs to follow, the governing equations are discretized from partial differential form to furnish a set of discrete equations. These may then be solved over a pipe network to compute pressures, flows and densities.

3.1 Mass equation

Mass conservation at a node i is enforced as follows (Greyvenstein and Laurie, 1994):

$$\sum_{j=1}^{J} s_{i,j}\rho_{i,j}Q_{i,j} = -d_i \tag{4}$$

where $i = 1,2,\ldots I$, with I denoting the total number of nodes in the mesh. In the above relation, summation is implied over all pipe branches j connected to node i, while the subscript i, j denotes a branch with local node numbers i and j. Further, $Q_{i,j}$ is the volume flux in pipe i,j and d_i is the external mass flow into node i. Finally:

$$s_{i,j} = \begin{bmatrix} 1 & \text{if flow enters the node} \\ -1 & \text{if the flow exits the node} \end{bmatrix}$$

Equation (4) is to be satisfies at every node in the pipe network.

3.2 Momentum equation

The momentum equation is discretized over the arbitrary 1D element shown in Figure 1. To achieve this, it is necessary to cast the equation into weak form and obtain analytical expressions for the resulting area integrals. This is detailed next.

Equation (2) is integrated over the control volume in Figure 1 as follows:

$$\int_V \frac{\partial}{\partial x}(p)\mathrm{d}V + \int_V \frac{\partial}{\partial x}(\rho u^2)\mathrm{d}V = \xi_v \tag{5}$$

where V denotes the total volume of the element and:

$$\xi_v = \int_V s_{i,j} H_{i,j} c_{f_{i,j}} u_{i,j}^2 \mathrm{d}V$$

The latter constitutes an element average source term.

Applying the Divergence Theorem to the volume integrals, the following expression now results:

$$\oint_A p n_x \mathrm{d}A + \oint_A \rho u^2 n_x \mathrm{d}A = \xi_V \quad (6)$$

where the pipe bounding area $A = A_i \cup A_j \cup A_s$. Here, the subscripts i and j denote the two surfaces through flow enters and leaves the pipe while s is the pipe enclosing surface. Further, n_x is the component of the outward pointing surface normal unit-vector in the direction of the pipe axisymmetric axis.

The first term on the left-hand-side of equation (6) will now be expanded as follows:

$$\oint_A p n_x \mathrm{d}A = \oint_{A_j} p n_x \mathrm{d}A + \oint_{A_i} p n_x \mathrm{d}A + \oint_{A_s} p n_x \mathrm{d}A \quad (7)$$

where the third term on the right-hand-side is in the interim set as:

$$\oint_{A_s} p n_x \mathrm{d}A = \beta$$

Noting that p is the average static pressure over the element flow cross-section, the remaining terms on the right-hand-side may be evaluated as:

$$\oint_A p n_x \mathrm{d}A = p_j A_j - p_i A_i + \beta \quad (8)$$

The second term in equation (6) is now similarly evaluated as:

$$\oint_A \rho u^2 n_x \mathrm{d}A = \rho_j u_j^2 A_j - \rho_i u_i^2 A_i \quad (9)$$

After substituting equations (8) and (9) into equation (6), an expression for the momentum equations is obtained:

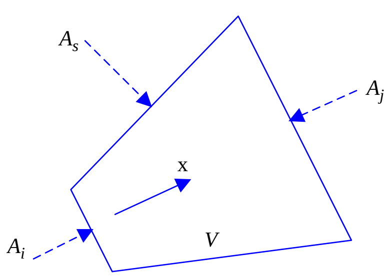

Figure 1.
Element over which the discretization takes place

$$p_j A_j - p_i A_i + \beta + \rho_j u_j^2 A_j - \rho_i u_i^2 A_i = \xi_V \tag{10}$$

If we base c_{f} upon A_j, the expression for ξ_V becomes:

$$\xi_V = s_{i,j} H_{i,j} c_{\mathrm{f}_{i,j}} u_{i,j}^2 A_j L_{i,j} \tag{11}$$

where $s_{i,j}$ is defined as before and $L_{i,j}$ is the element length.

The above semi-discrete equation is not suitable for solution in the current form as the static pressure across a branch connection (node) with minimal frictional losses (assumed in this work) is not constant. This is a hindrance as a single pressure value is calculated at a node. This may however be circumvented by solving for the total pressure at the nodes instead of the static pressure, as the former is constant across a branch connection by virtue of Bernoulli's equation (assuming negligible change in fluid density over a branch connection).

Following from the above, the total pressure may be written as the sum of the dynamic and static pressures as:

$$p_0 = p_{\mathrm{dyn}} + p_{\mathrm{s}} \tag{12}$$

where $p_{\mathrm{dyn}} = (1/2)\rho u^2$. Substituting the expression for static pressure into equation (11) results in:

$$p_{0j} A_j - p_{0i} A_i + \beta + \frac{1}{2}\left(\rho_j u_j^2 A_j - \rho_i u_i^2 A_i\right) = \xi_V \tag{13}$$

Note that the concept of total pressure is implemented in such a way that no assumption regarding compressibility across an element is made.

We now return to the β-term, which accounts for the change in static pressure over an element due to change in pipe flow area. From Figure 1 and Bernoulli, we may obtain the following expression for the pressure from the definition of total pressure for an incompressible fluid:

$$p(x) = p_{0i} - \frac{1}{2}\frac{\rho_i^2}{\rho_j}\frac{Q_i^2}{A^2(x)} \tag{14}$$

where Q_i and p_{0i} are the volume flow and total pressure at node i. Substituting equation (14) into the expression for β and evaluating the integral over the element analytically, the following results:

$$\beta = \oint_{A_s} p n_x \mathrm{d}A = -1\left(p_{0i}(A_j - A_i) + \frac{1}{2}\frac{\rho_{\mathrm{i}}^2}{\rho_j} Q_i^2 \left(\frac{1}{A_j} - \frac{1}{A_i}\right)\right) \tag{15}$$

Note that equation (15) is zero in the case of a constant area duct. The implication is that the above-discrete expressions may be applied to both constant and variable cross sectional area ducts in the case of incompressible flow, and only constant flow area ducts in the case of compressible flow.

The following fully discretized expression for the momentum equation now results:

$$\Delta p_{0i,j} = p_{0j} - p_{0i} = s_{i,j} c_{f_{i,j}} u_{i,j}^2 + \frac{\rho_i^2 Q_i^2}{2\rho_j A_j}\left(\frac{1}{A_j} - \frac{1}{A_i}\right) - \frac{1}{2A_j}\left(\rho_j A_j u_j^2 - \rho_i A_i u_i^2\right) \quad (16)$$

For incompressible flows, applicability is guaranteed to variable area ducts with geometrically complex features such as sudden expansions, as no simplifying assumption has been made in the derivation with regards to the element-wise static pressure distribution. Equation (16) is however not directly solvable in its present form as it contains nodal values for quantities such as flow and density, which are not solved for with the hybrid pipe network approach. As an objective is to solve for the elemental flow $Q_{i,j}$, we need to obtain an expression for the elemental and element in and out flow velocities ($u_{i,j}$, u_i and u_j) in terms of the variables solve for.

The elemental velocity $u_{i,j}$ is merely the elemental flow divided by the mean elemental cross sectional area:

$$u_{i,j} = \frac{Q_{i,j}}{A_{i,j}} \quad (17)$$

The velocity u_a is calculated from Q_a in a similar manner where $a = \{i, j\}$. Further, Q_a is also not explicitly solved for and must be calculated as a function of $Q_{i,j}$, which may be obtained through the conservation of mass-flow over an element. This implies that the nodal densities ρ_i and ρ_j need to be solved simultaneously with Q_a. From mass conservation, the nodal velocities local to an element i, j are calculated as:

$$u_a = \frac{\rho_{i,j} Q_{i,j}}{\rho_a A_a} \quad (18)$$

where $a = \{i, j\}$. However, ρ_a may be a function of u_a, which is in turn related to static pressure at node a. The relation for ρ_a in terms of u_a and p_{0a} is given by:

$$\rho_a = \frac{\delta_{ag}}{RT_a}\left(p_{0a} - \frac{1}{2}\rho_a u_a^2\right) + (1 - \delta_{ag})\rho_{al}(T) \quad (19)$$

The elemental density is taken as the linear average of the nodal densities:

$$\rho_{i,j} = \frac{1}{2}(\rho_j + \rho_i) \quad (20)$$

The above density interpolation expression is second order accurate, which is in-line with the overall accuracy of the hybrid discretization scheme. Finally, equations (18) and (19) need to be solved simultaneously via numerical iteration to obtain ρ_a and u_a for a given p_{0a}.

After implementing the above expressions into equation (16), the following results:

$$\Delta p_{0i,j} = s_{i,j} H_{i,j} c_{f_{i,j}} Q_{i,j}^2 + \frac{\rho_{i,j}^2}{2\rho_j A_j}\left(\frac{1}{A_j} - \frac{1}{A_i}\right) Q_{i,j}^2 - \frac{\rho_{i,j}^2}{2A_j}\left(\frac{1}{\rho_j A_j} - \frac{1}{\rho_i A_i}\right) Q_{i,j}^2 \quad (21)$$

which is now written in terms of variables which are explicitly solved for. This equation constitutes the discretized form of the momentum equation and describes compressible gas and incompressible gas and liquid steady flows in constant area ducts as well as incompressible flow in variable area ducts. It is to be satisfied over each element.

4. Pressure correction methodology

As per Greyvenstein and Laurie (1994), the first step in the solution process is the construction and solution of a so-called pressure correction matrix. The calculated pressure correction values are used to compute the corrected pressure values as follows:

$$p_{0i} = \alpha p^{*}_{0i} + p'_{0i} \tag{22}$$

where the superscripts * and $'$, respectively, denote the current approximate solution and the correction. Further, α is the pressure correction relaxation factor. The construction of an equation for the pressure correction commences by substituting the following relations for flow and density:

$$Q_{i,j} = Q^{*}_{i,j} + Q'_{i,j} \tag{23}$$

$$\rho_{i,j} = \rho^{*}_{i,j} + \rho'_{i,j} \tag{24}$$

into the continuity equation (equation (4)) which results in:

$$\sum_{j=1}^{J} s_{i,j}\left(\rho^{*}_{i,j}Q^{*}_{i,j} + \rho'_{i,j}Q^{*}_{i,j} + \rho^{*}_{i,j}Q'_{i,j}\right) = -d_i \tag{25}$$

Here, the density-flow correction term, $\rho'_{i,j}Q'_{i,j}$, has been omitted as is becomes insignificant as the solution process converges (Greyvenstein and Laurie, 1994).

Equations (22) and (25) are coupled via a relationship between the pressure correction and the flow correction. This is accomplished by differentiating the discretized pressure drop-flow equation (equation (21)) with respect to the element flow. Before the equation is differentiated, it is advantageous to rewrite it in the following form:

$$p_{0j} - p_{0i} = Q^{2}_{i,j} \cdot \varphi_{i,j} \tag{26}$$

where:

$$\varphi_{i,j} = s_{i,j}H_{i,j}c_{\mathrm{f}_{i,j}} + \frac{\rho^{2}_{i,j}}{2\rho_j A_j}\left(\frac{1}{A_j} - \frac{1}{A_i}\right) - \frac{\rho^{2}_{i,j}}{2A_j}\left(\frac{1}{\rho_j A_j} - \frac{1}{\rho_i A_i}\right)$$

Equation (26) is now differentiated with respect to the element flow:

$$\frac{\partial p_{0j}}{\partial Q_{i,j}} - \frac{\partial p_{0i}}{\partial Q_{i,j}} = s_{i,j}H_{i,j}2Q_{i,j}\varphi + s_{i,j}H_{i,j}Q^{2}_{i,j}\frac{\partial \varphi_{i,j}}{\partial Q_{i,j}} \tag{27}$$

Because the partial differential terms ∂() on the left-hand-side will become zero as convergence is reached, they may be replaced by the correction term ()′:

$$\frac{p'_{0j}}{Q'_{i,j}} - \frac{p'_{0i}}{Q'_{i,j}} = s_{i,j} H_{i,j}\left(2Q_{i,j}\varphi + Q^{2}_{i,j}\frac{\partial\varphi}{\partial Q_{i,j}}\right) \tag{28}$$

Provided that the Jacobean term $\partial\varphi/\partial Q_{i,j}$ is known, this expression for the flow-correction in terms of the pressure-correction (which is applicable to both compressible and incompressible flows) is viewed as simple and easily implementable into computer code. A further advantage of this approach is that flow-related nonlinearities such as the c_{f} coefficient are automatically taken in consideration. This will be shown to have a significant effect on convergence performance.

To complete the proposed algorithm, $\partial\varphi/\partial Q_{i,j}$ is easily computed numerically to first order accuracy as follows:

$$\frac{\partial\varphi}{\partial Q_{i,j}} = \frac{\varphi(Q_{i,j} + \mathrm{d}Q_{i,j}) - \varphi(Q_{i,j})}{\mathrm{d}Q_{i,j}} \tag{29}$$

where:

$$\mathrm{d}Q_{i,j} = \max\left(10^{-3}Q_{i,j},\;\; 10^{-5}Q^{\max}_{i,j}\right)$$

The latter expression keeps $dQ_{i,j}$ from becoming zero.

The effect of the order of accuracy of equation (29) on solution accuracy and convergence characteristics was found to be negligible. The cost of computing the Jacobean term was also found to be insignificant in terms of the scheme's overall CPU cost, as the bulk of the computational effort is expended on inverting the pressure correction matrix.

Through rearranging the terms of equation (28), an equation for the flow correction in terms of pressure correction is now established as:

$$Q'_{i,j} = \frac{p'_{0j} - p'_{0i}}{s_{i,j}H_{i,j}\left(2Q_{i,j}\varphi + Q^{2}_{i,j}(\partial\varphi/\partial Q_{i,j})\right)} \tag{30}$$

The density correction may be obtained via equation (20) as follows:

$$\rho'_{i,j} = \frac{1}{2}(\rho'_j + \rho'_i) \tag{31}$$

Finally, the expression for the pressure correction in terms of the flows and the densities may be found by substituting equations (23), (24), (30) and (31) into equation (25). The pressure correction values are now solved simultaneously at all nodes in the network via LU decomposition. The flows and densities may subsequently be calculated by means of equations (22), (30), (23), (31) and (24). Figure 2 shows the numerical solution procedure diagrammatically.

5. Convergence and stability

For the nodal method to yield accurate results, two convergence parameters are employed (Greyvenstein and Laurie, 1994). The first one verifies the extent of convergence of the continuity equation (equation (4)) and the other that of the pressure

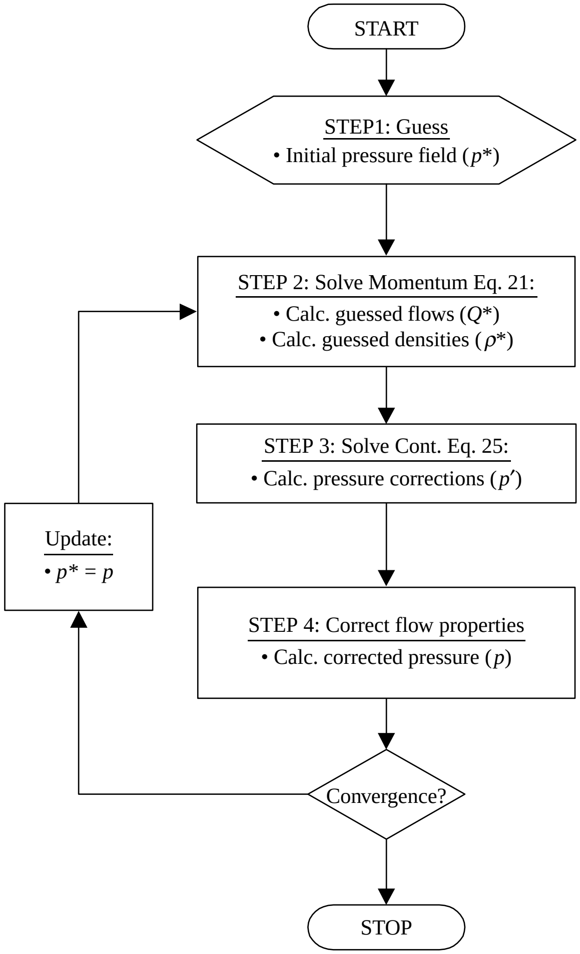

Figure 2.
Numerical computational scheme

drop-flow rate equation (equation (21)). The convergence parameter for the former is defined as:

$$\varepsilon_{\mathrm{Continuity}} = \frac{\left| \sum_{j=1}^{J} (s_{i,j}\rho_{i,j}Q_{i,j}) + d_i \right|_{\max}}{\left(\left(\sum_{i=1}^{I} \sum_{j=1}^{J} |s_{i,j}\rho_{i,j}Q_{i,j}|_i \right) / E \right)} \tag{32}$$

where max is the maximum value in the network and E the total number of elements. The convergence parameter for the pressure drop-flow rate equation is defined as:

$$\varepsilon_{\mathrm{Pressure\,drop}} = \sum_{e=1}^{E} \left| \frac{\Delta p_{\mathrm{PFE}} - \Delta p_{\mathrm{Nodal}}}{\Delta p_{\mathrm{PFE}}} \right| \tag{33}$$

where Δp_{PFE} is the total pressure drop across an element and $\Delta p_{\mathrm{Nodal}}$ is the difference in total pressure between the two nodes linked to the element. Convergence to engineering accuracy is established when $\varepsilon < 10^{-4}$.

6. Numerical tests and discussion

The developed numerical procedure is tested against three problems. The first two are compressible flow systems used by Greyvenstein and Laurie (1994) and Greyvenstein (2002). These problems were selected due to the latter papers employing a similar numerical scheme. The third test case involves the incompressible liquid flow through a variable cross-sectional duct viz. a sudden expansion.

6.1 Compressed air network

Greyvenstein and Laurie (1994) published a compressed air network example in their paper to demonstrate the performance of their method. The developed algorithm will now be used to analyse this network in order to verify accuracy. Figure 3 shows the layout of the network with boundary conditions. The element-related data may be found in Greyvenstein and Laurie (1994).

The boundary conditions to this network are inlet or supply pressures of 600 kPa, while the outlet or discharge pressures are set equal to 300 kPa. The supply pressures are applied to nodes one and 14, and the discharge pressures are applied to all nodes with only one connecting element. The friction factor is initially fixed to $f = 0.03$ as per

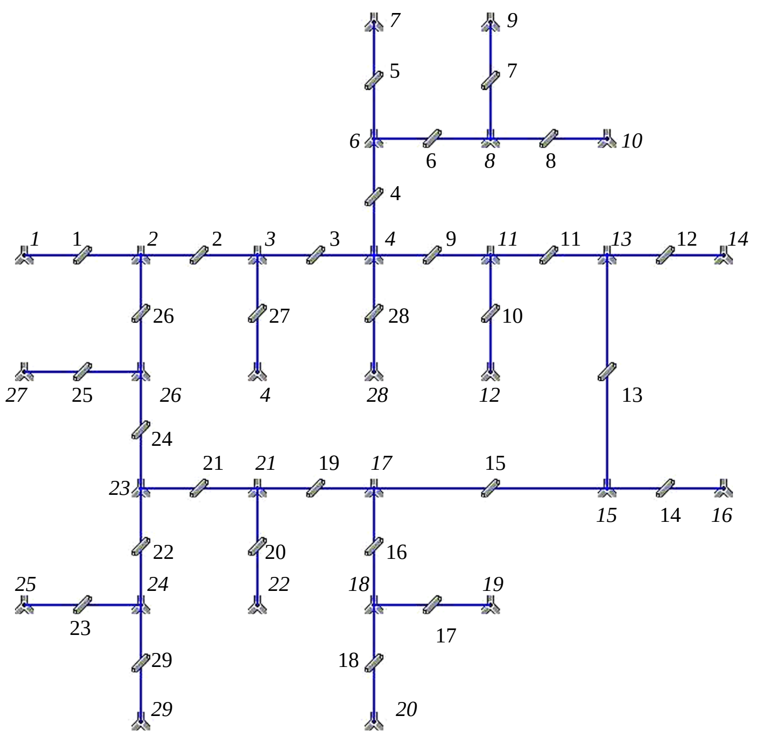

Figure 3.
Compressed air network

the aforementioned paper. The temperature field has been kept constant at 15°C with no heat addition or subtraction. The relaxation factor was set to 1.0.

The solved pressures and flows are shown in Table I (constant friction network) and compare well with the results of Greyvenstein and Laurie. The convergence history of the solution process is shown in Figure 4. The initial residual is different from that of the other authors which is thought to be due to different initial guessed values employed. In this work guessed nodal pressures were used, the values of which were chosen just below the highest specified pressure in the network (automatically calculated by the solver). Convergence to engineering accuracy ($\log(\varepsilon_p) = -4$) was however reached within eight iterations, which is similar to that of the other authors. The proposed formulation therefore offers similar accuracy and performance.

In real pipes, friction is however a function of the flow rate and not fixed as previously simulated. Therefore, the analysis of the same compressed air pipe network was repeated with friction values as a function of the flow $f(Q)$ through the network. This analysis was also used to evaluate the effect on convergence of taking the friction factor as a function of

Table I.
Results of the simulation package for the compressed air network

	Constant friction network ($f = 0.03$)				Variable friction network		
	Published (Patankar, 1980)		This work		This work		
No.	Mass flow (kg/s)	Pressure (kPa)	Mass flow (kg/s)	Pressure (kPa)	Mass flow (kg/s)	Pressure (kPa)	f
1	0.01646	600.00	0.01645	600.00	0.03109	600.00	0.008
2	0.00803	521.51	0.00803	521.51	0.01517	529.37	0.009
3	0.00360	411.34	0.00360	411.37	0.00663	419.93	0.010
4	0.00338	300.00	0.00337	300.00	0.00610	300.00	0.009
5	0.00178	385.50	0.00178	385.53	0.00328	390.66	0.011
6	0.00159	320.57	0.00159	320.58	0.00282	324.93	0.011
7	0.00080	300.00	0.00080	300.00	0.00141	300.00	0.013
8	0.00080	304.23	0.00080	304.23	0.00141	305.91	0.013
9	−0.00360	300.00	−0.00360	300.00	−0.00663	300.00	0.010
10	0.00444	300.00	0.00443	300.00	0.00855	300.00	0.009
11	−0.00803	411.34	−0.00803	411.37	−0.01517	419.93	0.009
12	0.01646	300.00	0.01645	300.00	0.03109	300.00	0.008
13	0.00843	521.51	0.00842	521.51	0.01592	529.37	0.008
14	0.00413	600.00	0.00413	600.00	0.00802	600.00	0.009
15	−0.00429	398.49	−0.00429	398.51	−0.00790	408.65	0.010
16	0.00280	300.00	0.00280	300.00	0.00513	300.00	0.010
17	0.00140	359.77	0.00140	359.78	0.00256	366.92	0.012
18	0.00140	312.86	0.00140	312.87	0.00256	316.43	0.012
19	−0.00149	300.00	−0.00149	300.00	−0.00277	300.00	0.013
20	0.00299	300.00	0.00299	300.00	0.00553	300.00	0.010
21	0.00149	354.80	0.00149	354.82	0.00277	359.86	0.013
22	0.00280	300.00	0.00280	300.00	0.00513	300.00	0.010
23	0.00140	359.77	0.00140	359.78	0.00256	366.92	0.012
24	0.00429	312.86	0.00429	312.87	0.00790	316.43	0.010
25	0.00413	300.00	0.00413	300.00	0.00802	300.00	0.009
26	0.00843	398.49	0.00842	398.51	0.01592	408.65	0.008
27	0.00444	300.00	0.00443	300.00	0.00855	300.00	0.009
28	0.00382	300.00	0.00382	300.00	0.00715	300.00	0.009
29	0.00140	300.00	0.00140	300.00	0.00256	300.00	0.012

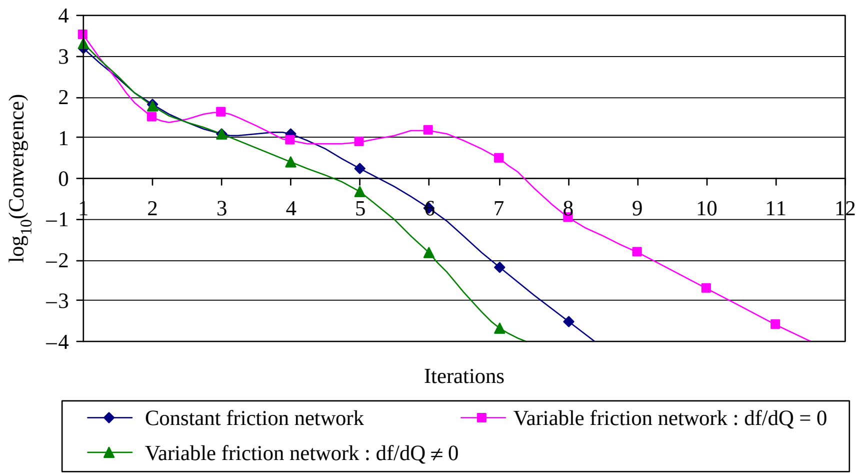

Figure 4. Convergence plots for the compressed air network simulation

the flow ($f(Q)$) when constructing the pressure correction matrix. The surface roughness was set to $e = 0.001$ mm for all the pipes, which corresponds to that of drawn tubing, and the Colebrook (1939) correlation employed to relate flow rate to frictional losses. All the other properties and conditions were as per the previous analysis.

For the first simulation in which the friction f was kept constant when constructing the pressure correction equation ($\mathrm{d}f/\mathrm{d}Q = 0$), the relaxation factor was kept at 1.0 and convergence to engineering accuracy was reached in 11 iterations as shown in Figure 4. The simulation was then repeated, and this time the friction factor was taken as a function of the flow when constructing the pressure correction matrix ($\mathrm{d}f/\mathrm{d}Q \neq 0$). Convergence was now reached in seven iterations. Note that the solved pressures and flows for both construction methodologies were identical and is given in Table I.

In the light of the above, it can be concluded that the proposed methodology offers similar performance compared to that of the other hybrid formulation in terms of both accuracy and convergence characteristics. It is also demonstrated that all types of flow-related nonlinearities should be taken into consideration when constructing the pressure correction matrix as this may have a significant effect on convergence. The proposed methodology facilitates this in a natural manner.

6.2 Isothermal steady-state compressible flow through a 100 m long pipeline

As noted above, the steady-state compressible flow benchmark case employed in Greyvenstein (2002) refers. This test case involves a 100 m long pipeline with a diameter of 0.5 m. Helium flows through the pipeline with a total outlet pressure of 200 kPa and an inlet temperature of 300 K. The friction factor is assumed to be constant at $f = 0.02$. The results of Greyvenstein, as well as an "analytical" solution obtained via a fourth order Runga Kutta numerical integration procedure of the following equation set (Zucrow and Hoffman, 1976), will be used for validation purposes:

$$\frac{\mathrm{d}M}{M} = \frac{(1 + 0.5(\gamma - 1)M^2)}{1 - M^2}\left\{\frac{\gamma M^2}{2}\left(\frac{f\,\mathrm{d}x}{D}\right) + \frac{(1 + \gamma M^2)}{2}\,\frac{\mathrm{d}T}{T}\right\} \tag{34}$$

where M and γ are respectfully Mach number and specific heat ratio.

The additional flow properties may be obtained from the following formulations (Zucrow and Hoffman, 1976):

$$\dot{m} = \mathrm{ApM}\sqrt{\frac{\gamma}{\mathrm{RT}}\left(1+\frac{\gamma-1}{2}M^2\right)} \tag{35}$$

$$\frac{P}{p} = \left(1+\frac{\gamma-1}{2}M^2\right)^{\gamma/(\gamma-1)} \tag{36}$$

$$\frac{T}{t} = \left(1+\frac{\gamma-1}{2}M^2\right) \tag{37}$$

where the properties in uppercase refers to the stagnation condition and in lowercase to the static condition.

The performance of the developed numerical method was evaluated by comparing predicted flows and the required number of elements to that of the others. In this work we employ ten elements to discretize the pipeline, as opposed to the 20 elements used by the other author. The inlet and outlet total pressure ratios obtained via the various algorithms as a function of the outlet Mach number is shown in Figure 5. The described method therefore furnished similar results as compared to the other author. This deems the equation set employed in this work as more accurate, as half the number of elements are required.

Table II documents the convergence statistics for different relaxation factor values and outlet Mach numbers for this test case. It is clear that in general, the lower the relaxation factor the more stable the method, however, the number of required iterations increases dramatically (more than twice that of the highest relaxation factor in almost all the cases). A reasonable trade-off between stability of the method and the cost of computation was found to be a relaxation factor of 1.0.

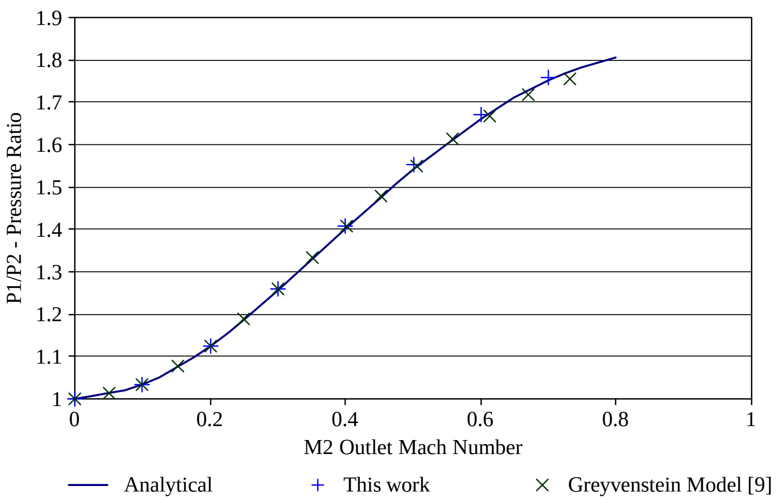

Figure 5.
Inlet to outlet pressure ratio as a function of outlet Mach number for steady isothermal flow in a 100 m long pipe line

6.3 Flow through a sudden expansion

The final test case is aimed at demonstrating the developed modelling technology in terms of capability to, in addition to accurately describing compressible flow, simulate incompressible flow with the added complexity of a discontinuously varying duct cross section. For this purpose, the sudden expansion incompressible flow problem described by White (1986) was modelled. A schematic of the test case is shown in Figure 6.

As shown, two reservoirs are connected by cast-iron pipes of varying diameters, which are joined abruptly, with sharp-edged entrance and exit. Including minor losses, the water flow rate is to be calculated if the difference in water surface height between two reservoirs results in a pressure difference of 134.5 kPa.

The following data for the pipes, entrance and exit were employed:

- Surface roughness = 0.04572 mm;
- Entrance loss coefficient = 0.5;
- Exit loss coefficient = 1;
- Lengths both = 6.096 m; and
- Pipe diameters = da = 0.0254 m and db = 0.0508 m.

Figure 7 shows how the problem was modelled via the developed simulation package where:

M2	Relaxation factor 0.5	0.8	1	1.2
0.1	16	9	7	Unstable
0.2	18	10	7	7
0.3	20	12	9	6
0.4	22	13	10	8
0.5	23	14	11	9
0.6	28	18	13	11
0.7	32	19	14	12

Table II. Number of required iterations of the proposed pipe network method for different Mach numbers and relaxation factors for the isothermal pipeline

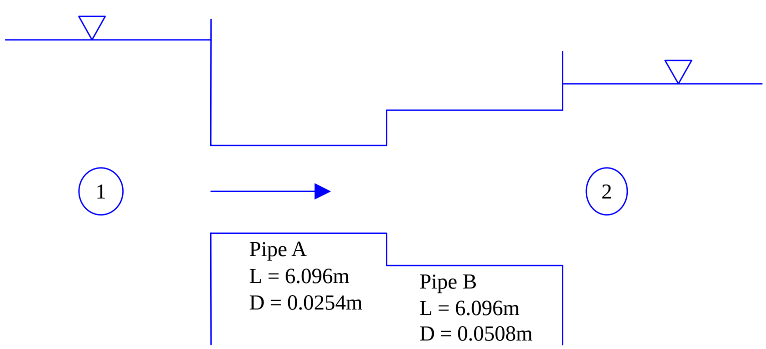

Figure 6. Sudden expansion problem

- Element 1 = entrance
- Element 2 = pipe A
- Element 3 = sudden expansion
- Element 4 = pipe B
- Element 5 = exit.

The flow predicted by the proposed method was 0.003262 m^3/s, which is within 3 percent of the published value (White, 1986). This result was obtained within 15 iterations as shown in the convergence plot (Figure 8) with a relaxation factor of 0.5. The capability of the proposed scheme to model incompressible flow through ducts with discontinuous varying cross-sections is therefore demonstrated.

7. Conclusion

A single equation set methodology for modelling both compressible gas and incompressible gas and liquid flow in pipe networks is proposed. In the latter case, the scheme is capable of modelling flow in ducts with discontinuously varying cross-sections. This model was found to yield results of similar accuracy as compared to that of others. In the case of a compressible flow problem, fewer elements were required as compared to recent work by others. It can therefore be concluded that this single equation set network model holds potential for solving a number of problems involving both gas and liquid flows, accurately and efficiently.

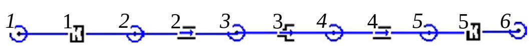

Note: Sudden expansion model

Figure 7.

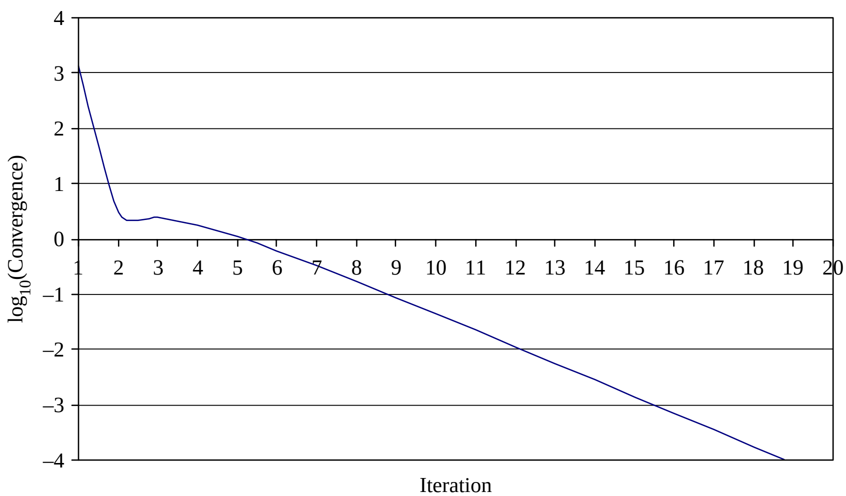

Figure 8.
Convergence plot for the sudden expansion

References

Colebrook, C.F. (1939), "Turbulent flow in pipes, with particular reference to the transition region between the smooth and rough pipe laws", *J. Instn. Civ. Engrs.*, Vol. 11, p. 133.

Greyvenstein, G.P. (2002), "An implicit method for the analysis of transient flows in pipe networks", *International Journal for Numerical Methods in Engineering*, Vol. 53, pp. 1127-43.

Greyvenstein, G.P. and Laurie, D.P. (1994), "A segregated CFD approach to pipe network analysis", *International Journal for Numerical Methods in Engineering*, Vol. 37, pp. 3685-705.

Osiadacz, A.J. (1987), *Simulation and Analysis of Gas Networks*, J.W. Arrowsmith Ltd, Bristol.

Osiadacz, A.J. (1988), "Methods of steady state simulation of a gas network", *International Journal of Systems Sciences*, Vol. 19 No. 11, pp. 2395-405.

Patankar, S.V. (1980), *Numerical Heat Transfer and Fluid Flow*, Hemisphere Publishing Co., Washington, DC.

Potter, M.C. and Wiggert, D.C. (1991), *Mechanics of Fluids*, Prentice-Hall, Englewood Cliffs, NJ.

Pretorius, J.J. (2004), "A network approach for the prediction of flow and flow splits in a gas turbine combustor", master's degree dissertation, University of Pretoria, Pretoria.

Stuttaford, P.J. and Rubini, P.A. (1996), "Prelimanary gas turbine combustor design using a network approach", Transactions of ASME, Paper No. 96-GT-135.

White, F.M. (1986), *Fluid Mechanics*, 2nd ed., McGraw-Hill, New York, NY.

Zucrow, M.J. and Hoffman, J.D. (1976), *Gas Dynamics*, Vol. 1, Wiley, New York, NY.

Corresponding author
A.G. Malan can be contacted at: a.g.malan@up.ac.za